THE ASTROPHYSICAL JOURNAL, 451:525–532, 1995 October 1

MERGERS OF DISSIPATIONLESS SYSTEMS: CLUES ABOUT THE FUNDAMENTAL PLANE

H. V. CAPELATO,[1] R. R. DE CARVALHO,[2,3,4] AND R. G. CARLBERG[5]

Received 1994 September 12; accepted 1995 April 12

ABSTRACT

We report the results of a set of simulations that were designed to study the physical properties of the "fundamental plane" (FP) of elliptical galaxies. By starting with two similar king models and varying the orbital energy and angular momentum, we have investigated the global properties of the remnants. The characteristic parameters of the end products seem to follow closely the observed FP. This trend was confirmed by a subsequent set of simulations in which merger remnants were merged among themselves; that is, merging of objects in the FP produces a new object in the FP. We find that the small departure from the virial theorem, which is characteristic of the fundamental plane correlations, is explained by the nonhomologous nature of the remnants. The simulated FP has a very small intrinsic scatter: compared to the observed one it enables us to establish that the central potential W_0 and the mass of the primordial units from which galaxies were formed could not have very broad distributions, although this is not a unique way to explain the difference in scatter between the predicted and the observed fundamental planes. Even though merging is selective (not all cosmological reasonable orbits merge), it cannot completely erase initial conditions. In other words, given appropriately correlated primordial units, subsequent merging will maintain a fundamental plane. Therefore, under the "dissipationless" approximation here, the FP should be independent of redshift (except for the evolution of their stellar populations) even if substantial merging has occurred.

Subject headings: galaxies: elliptical and lenticular, cD — galaxies: interactions — galaxies: kinematics and dynamics — methods: numerical

1. INTRODUCTION

The last decade has witnessed the growing of our understanding of the global properties of galaxies. In particular, the accumulation of high-quality photometric and kinematic data for ellipticals has revealed that these systems form a two-parameter family in the space defined by radius (R), surface brightness (I), and velocity dispersion (σ) (Djorgovski & Davis 1987; Dressler et al. 1987; Djorgovski & de Carvalho 1990). The relation involving such quantities is called the "fundamental plane" (FP). The observed FP can be described as $R \sim \sigma^A I^B$, where $A \sim 1.4$ and $B \sim -0.9$ (e.g., Djorgovski 1992). Assuming homology, for a pure virial theorem we should have $R \sim \sigma^A I^B (M/L)^{-1}$ from which follows $(M/L) \sim M^{1/6}$ (Faber et al. 1987; Djorgovski 1988). One of the possible consequences of this result is that the formation of elliptical galaxies was partly dissipative, otherwise we should not expect any relation between (M/L) and mass. Other possibilities like the presence of dark matter or varying IMF can also be claimed as reasonable explanations for such dependence (cf. Renzini & Ciotti 1993; Djorgovski & Santiago 1993).

Recent papers have addressed the study of the structural and dynamical properties of early-type galaxies, exploring the physical meaning of the FP and what we can learn about galaxy formation by probing its characteristics (e.g., Djorgovski 1992; Bender, Burstein, & Faber 1992; Hernquist, Spergel, & Heyl 1993; Bertin & Stiavelli 1993). Bender et al. (1992) defined a new set of variables to study the properties of the FP, which are combinations of R, σ, and I. They propose that within this new three-space, the physical processes related to the formation and evolution of ellipticals are better displayed. One of their basic assumptions is that ellipticals can be understood as homologous systems. However, Caon, Capaccioli, & D'Onofrio (1993), by carefully inspecting the major-axis luminosity profiles of a sample of early-type galaxies, found that this may not be the case. This poses a serious problem for the study of the FP as a fundamental tool to probe mechanisms of galaxy formation.

One of the first papers to deal with the question of whether or not merging can preserve homology was Farouki & Shapiro (1982) and Farouki, Shapiro, & Duncan (1983, hereafter FSD). The basic conclusion from their experiment is that the remnant galaxies strongly deviate from homology with their initial models. Using their relations it is possible to recover the observed FP. Navarro (1989) also discusses the nonhomology problem, although he does not focus on this aspect of the interpretation of the FP.

The aim of this paper is to study whether or not the nonhomologous nature of the merger remnants can at least partly explain why the FP deviates from a pure virial theorem. In § 2 we give basic elements of our numerical experiment, and § 3 presents the main results regarding the properties of the FP. Finally, in § 4 we discuss the nonhomologous nature of the remnants of the simulations studied here.

2. SIMULATIONS SETUP

The initial model galaxies used in the experiments reported here are 4096 particle Monte Carlo realizations of a spherical isotropic King model generated with central potential $W_0 = 5$ (concentration $c = \log r_t/r_c = 1.03$; see King 1966). Although the concentration parameter is too low compared to real elliptical galaxies, we expect that such a value does not restrict any of our results.

[1] Div. de Astrofísica—INPE/MCT, C.P. 515, S. José dos Campos. 12201-970, Brazil.
[2] Instituto Astronômico e Geofísico, USP, C.P. 9638, São Paulo, 01065-970, Brazil.
[3] On leave of absence from Observatório Nacional–CNPq–DAF.
[4] Present Address: California Institute of Technology, 105-24, CA 91125.
[5] Department of Astronomy, University of Toronto, Toronto, M5S 1A1, Canada.

Mass and length units were set as $10^{10}\ M_\odot$ and 1 kpc, respectively; these values, together with $G = 1$, fix our time and velocity units as 4.72 Myr and 207 km s^{-1}, respectively. The initial models have total mass $M = 10$ (which means that the particle mass, m_p, is ~ 0.00244) and half-mass radius $r_h = 2$ in these units. The σ_* parameter, which characteristic of the kinetic temperature of the King models, amounts to 1.086 (225 km s^{-1}). Note that scaling to different values of M and r_h does not change any of our units but does change σ_* by a factor $(M/r_h)^{1/2}$.

The simulations were made using a C translation of the Barnes & Hut (1986) TREECODE, running on SUN Sparc2 machines. The code parameters were set as tolerance parameter, $\theta = 0.8$; time step $\Delta t = 0.025$; potential softening $\epsilon = 0.05$. The force computation includes quadrupole correction terms following Dubinski (1988).

We have approximately followed the formulation of Binney & Tremaine (1987) to characterize the initial orbital conditions of the encounters. We define the dimensionless energy and angular momentum of the initial orbit as $\hat{E} = E_{\rm orb}/(\frac{1}{2})\mu\sigma_*^2$ and $\hat{L} = L_{\rm orb}/\mu r_h \sigma_*$, where $\sigma_* = (\sigma_{*1} \times \sigma_{*2})^{1/2}$ and $r_h = (r_{h_1} \times r_{h_2})^{1/2}$. The indices denote each of the initial galaxies, and μ is the reduced mass of the system. For initial models other than King's, these definitions must be applied by substituting the σ_* parameter by some characteristic internal velocity dispersion of the model.

To fully determine the orbital elements of the encounter, a further dimensionless parameter must be defined:

$$A = \frac{2G(M_1 + M_2)}{r_h \sigma_*^2}.$$

Given a set of values of $\hat{E}$, $\hat{L}$, and A, the two-body orbit equation may be straightforwardly obtained by writing the orbital energy and angular momentum as a function of the center-of-mass positions and velocities of the pair, thus allowing the choice of the initial conditions for the encounter. We note in passing that the parameter A depends uniquely upon the internal structure of the initial interacting galaxies. Therefore, a comprehensive study of merger remnants as a function of the initial conditions should make use of a large set of numerical experiments spanning a physically reasonable range of ($\hat{E}$, $\hat{L}$, A). In this paper, we restrain ourselves to the plane defined by $A = 16.96$, given by the initial galaxy model described above. For comparison, the merger simulations described by Navarro (1989) have $A = 16.70$.

We have determined the initial separations and velocities for the encounters from a grid of values previously fixed in the ($\hat{E}$, $\hat{L}$, $A = 16.96$) plane. For bound initial orbits, these initial conditions were always taken at the apocenter position in order to maximize the dynamical effects of tidal forces between the companions. For unbound orbits, the initial conditions were taken such that the separations were ~ 2 times the tidal radius of the galaxies, which amounts to 10.7 kpc. Table 1 summarizes the initial conditions and characteristic parameters of the simulations discussed in this paper. Column (1) lists the label of each run, which will be described below. Columns (2) and (3) give the initial orbital energy and angular momentum, as defined above. Columns (4)–(6) give the center-of-mass separations and the radial and tangential velocities at the beginning of the simulations. The predicted time interval before the two-body pericenter, $T_{\rm per}$, and the crossing times of the final objects, $T_{\rm cr} = GM^{5/2}/(2E)^{3/2}$, where M and E are, respectively, the total mass and energy of the systems, are given in columns (7) and (8). Column (9) gives the total time elapsed up to the end of the simulation in crossing time units. In all cases, the simulation was stopped at $30T_{\rm cr}$, after the first peri-

TABLE 1

PARAMETERS OF THE SIMULATIONS

Run (1)	$\hat{E}$ (2)	$\hat{L}$ (3)	Separation (4)	$v_{\rm rad}$ (5)	$v_{\rm tan}$ (6)	$T_{\rm per}$ (7)	$T_{\rm cr}$ (8)	$T_{\rm end}/T_{\rm cr}$ (9)	log r_e (10)	$\langle \mu_e \rangle$ (11)	log σ_0 (12)
R1	0	0	15.0	−1.63	0.00	6.1	6.84	44.4	0.36 ± 0.02	23.12 ± 0.07	2.39 ± 0.01
R2	−4	1	8.4	0.00	0.26	6.2	3.46	45.1	0.28 ± 0.02	22.62 ± 0.08	2.45 ± 0.02
R3	−3	1	11.2	0.00	0.19	9.5	4.04	30.2	0.32 ± 0.02	22.80 ± 0.10	2.43 ± 0.02
R4	−2	1	16.8	0.00	0.13	17.4	4.74	38.0	0.33 ± 0.01	22.91 ± 0.06	2.42 ± 0.01
R5	−1	1	33.8	0.00	0.06	49.1	5.59	39.9	0.35 ± 0.02	23.02 ± 0.07	2.40 ± 0.02
R6	+0.5	1	30.0	−1.39	0.07	15.5	7.65	31.9	0.39 ± 0.03	23.24 ± 0.13	2.39 ± 0.02
R7	−7.5	2	4.0	0.00	1.09	2.4	2.50	33.2	0.19 ± 0.02	22.16 ± 0.12	2.47 ± 0.03
R8	−5.7	2	5.4	0.00	0.80	3.6	2.86	29.7	0.22 ± 0.02	22.33 ± 0.12	2.45 ± 0.02
R9	−1	2	33.4	0.00	0.13	49.0	5.67	47.5	0.37 ± 0.02	23.12 ± 0.12	2.40 ± 0.02
R10	0	2	15.0	−1.61	0.29	6.4	6.84	30.1	0.38 ± 0.02	23.19 ± 0.10	2.39 ± 0.02
R11	+0.5	2	15.0	−1.78	0.29	6.0	7.80	48.0	0.41 ± 0.02	23.36 ± 0.10	2.39 ± 0.01
R12	−7.9	3	2.4	0.00	2.70	2.2	3.52	31.2	0.27 ± 0.03	23.57 ± 0.13	2.41 ± 0.02
R13	−6.9	3	3.4	0.00	1.93	2.7	2.88	30.9	0.23 ± 0.03	22.34 ± 0.15	2.42 ± 0.02
R14	−5.1	3	5.3	0.00	1.24	4.2	3.07	48.5	0.25 ± 0.03	22.44 ± 0.16	2.43 ± 0.01
R15	−2.8	3	10.9	0.00	0.60	10.4	4.11	44.8	0.32 ± 0.03	22.79 ± 0.14	2.41 ± 0.02
R16	−1	3	32.8	0.00	0.20	49.1	5.59	37.2	0.37 ± 0.03	23.09 ± 0.13	2.39 ± 0.01
R17	0	3	15.0	−1.57	0.43	6.7	6.84	37.0	0.40 ± 0.02	23.26 ± 0.12	2.38 ± 0.01
R17-17	+0.5	3	30.0	−1.74	0.37	12.6	13.38	30.0	0.70 ± 0.03	24.15 ± 0.16	2.41 ± 0.01
R6-6	−2	1	28.7	0.00	0.12	28.5	7.94	40.8	0.60 ± 0.04	23.56 ± 0.19	2.44 ± 0.03
R17-King1M	−4	1	11.6	0.00	0.24	8.4	5.10	32.0	0.44 ± 0.03	24.03 ± 0.17	2.46 ± 0.02
King 2-M	0	0	30.0	−1.63	0.00	12.2	13.60	32.0	0.66 ± 0.02	23.85 ± 0.07	2.40 ± 0.01
R9($W0 = 8$)	−1	2	31.5	0.00	0.14	45.1	5.09	38.9	0.42 ± 0.02	23.33 ± 0.10	2.41 ± 0.01
R3($W0 = 8$)	−3	1	10.6	0.00	0.21	8.7	3.67	32.5	0.32 ± 0.01	22.80 ± 0.07	2.44 ± 0.01
R9-9($W0 = 8$)	−2	2	26.1	0.00	0.33	25.0	6.77	33.7	0.63 ± 0.04	23.67 ± 0.21	2.47 ± 0.01
$2NW0 = 5$	−1	1	33.8	0.00	0.06	49.1	5.59	38.1	0.37 ± 0.03	23.12 ± 0.13	2.41 ± 0.01
$3NW0 = 8$	−3	1	10.5	0.00	0.22	8.7	3.69	32.5	0.34 ± 0.02	22.91 ± 0.12	2.44 ± 0.02

center encounter of the system, in order to guarantee that the central part of the remnants reached dynamical equilibrium (see also Navarro 1989). The surface density profiles at one specific projection were inspected at $25T_{cr}$ and $30T_{cr}$, and they exhibited no significant variations within r_h, attesting that equilibrium was reached in the central parts of the remnants. Columns (10), (11), and (12) list the effective radius (r_e), the mean surface brightness inside r_e ($\langle\mu_e\rangle$), and the central velocity dispersion (σ_0), for the merger remnant of each simulation. The relative variations of the total energy and angular momentum were typically below 0.5% and 1.5%, respectively, and the relative mass loss of remnants due to escapers was less than 10%.

The simulations were labeled as follows

1. Ri, $i = 1, 17$,—These are simulations of the encounter of similar King model galaxies described in the beginning of this section, where the index i represents a given pair of $(\hat{E}, \hat{L})$.

2. R6-6.—This is a simulation merging replicas of the end product of the R6 run. These replicas were constructed so as to keep the total number of particles in each object always bounded to 4096. We have adopted much the same strategy as FSD to obtain the replicas. For a remnant with N_p particles, after removing escapers, we recorded these particles in decreasing order of binding energy, defining the replicas by the positions and velocities of the odd-numbered and even-numbered particles. The particle mass was then doubled in order to ensure equilibrium.

3. R17-17.—This is the same as in simulation 2 but between replicas of R17. For this run the softening parameter was set at $\epsilon = 0.1$.

4. R17-King1M.—This is an encounter between the end product (not a replica) of the R17 run with the initial King model galaxy described before.

5. "King-2M."—This is an encounter between two similar King model galaxies with $W_0 = 5$ as in simulation 1, but with M and r_h doubled.

6. R9(W0 = 8) and R3($W0 = 8$).—These are similar to runs R9 and R3, but with initial King model galaxies of $W_0 = 8$ and the other input parameters unchanged.

7. R9-9($W0 = 8$).—This is a simulation merging the end product of the R9($W0 = 8$) run with itself. We have used the same replica scheme described above in item B.

8. "$2NW0 = 5$."—This is similar to R5, but the total number of particles per galaxy has been doubled (8192).

9. "$3NW0 = 8$."—This is similar to R3($W0 = 8$), but with the total number of particles per galaxy has been tripled (12,288). The softening parameter for this run was $\epsilon = 0.02$. These last two runs have integration time steps half as big as that for the others.

Our simulations do not explicitly include a luminous stellar component and an extended dark matter component. There are several arguments for this approach. First, we wish to establish the scaling properties of single-component dynamical systems before going on to two-component ones. An eventual goal is to do more general simulations with initial conditions drawn from larger scale cosmological simulations. The minimal goal of the simulations discussed here is to establish whether the merging of simple one component systems will destroy any preexisting FP relation. Second, these one-component systems are initiated in sufficiently close orbits that the physical interpretation is that they have already spiralled through the bulk of their dark halos. Furthermore, the effect of dark halos on the visible bodies is, crudely, equivalent to the visible bodies alone but arriving in contact on orbits which have been altered by the dark halos. Consequently, we conclude that investigating the merging of single-component systems with "vacuum" exteriors will be a useful guide to the question of how the FP transforms under merging.

3. THE FUNDAMENTAL PLANE OF THE MERGER REMNANTS

The merger remnants were analyzed so as to reproduce the quantities related to the observed FP of elliptical galaxies. Each remnant was projected in 100 random directions and, for each projection, the barycenter of the distribution was found and quantities like the effective radius r_e (defined as the radius of a circle encompassing half of the particles, $N_p/2$, where $N_p/2$ is the net number of particles after removing the escapers) and the mean surface density inside r_e, $\bar{\Sigma}_e = N_p m_p/2\pi r_e^2$, were measured. We defined a mean "surface brightness" as $\langle\mu_e\rangle = -2.5 \log \bar{\Sigma}_e + C$, the value of the constant, $C = 29$, is such as to allow this quantity to assume values about the same order as those typically measured in real galaxies. A projected central velocity dispersion, σ_0, was measured inside a square "slit" of side $f \times r_e$, as the mean square projected velocity of all particles inside the "slit." The median of these projected quantities (taken from the 100 projections) were then calculated and attributed to the remnant. The corresponding errors are standard deviations based on the quartiles of the distribution of each quantity. The characteristic parameters, r_e, σ_0, and $\langle\mu_e\rangle$ (measured for a slit with $f = 0.2$), for the end products of the simulations R1, ..., R17 were then combined in the same way as in Djorgovski & Davis (1987) and are shown in Figure 1 as

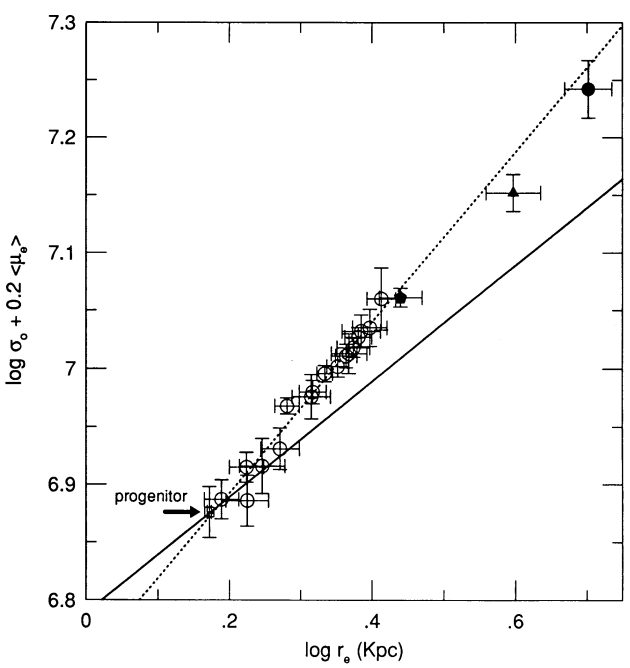

FIG. 1.—This figure shows the FP of the remnants for the numerical experiments R1–R17. Each remnant is plotted as an open circle; the open square (designated by an arrow marked "progenitor") represents the initial model galaxy for these runs, as described in the text. Second generation remnants are shown with filled symbols: (1) the two end-products with largest r_e (R6 and R17) were merged with their own replicas and are represented by a triangle, for the run R6-6, and a circle, for the run R17-17; (2) the solid pentagon represents the remnant of a merger between the "standard" King model galaxy ($W_0 = 5$) and the R17 end product. The solid line represents the virial relation and the dotted line the best-fit line to the points corresponding to the first generation remnants (runs R1–R17).

open circles. The factor 0.2 was established by looking at what observers usually take to measure the central velocity dispersion. From Davies et al. (1987) and Burstein et al. (1987) we estimate that $0.2r_e$ is the typical aperture size as far as the proper comparison between simulation and data is concerned. It is important to emphasize that Davies et al. (1987) is the most extensive list of central velocity dispersion available in the literature with 462 measurements. That was the main motivation why we used the aperture approach rather than fitting a Gaussian to the projected velocity dispersion profile, which is a difficult approach from the observational view point (there are less than 100 ellipticals for which reliable velocity dispersion profile is available). The solution which optimizes the correlation coefficients and the orthogonal least squares is (dotted line in Fig. 1):

$$\log r_e = (1.36 \pm 0.08)(\log \sigma_0 + 0.2\langle\mu_e\rangle) + C \,. \quad (1)$$

These coefficients are remarkably similar to those found for real elliptical galaxies in the K band (e.g., Recillas-Cruz et al. 1991). Our simulations trace the counterpart of the observed elliptical galaxies not significantly affected by dissipative processes as star formation induced by merging; that is why we compare our results with the infrared fundamental plane. The open square in Figure 1 represents the initial King model for the first 17 experiments presented in Table 1 and it was not included in the fit. We found the solution for the FP slightly dependent on the size of the slit used to measure σ_0. For instance, for a slit with $f = 0.5$ the coefficient 1.36 changes to 1.52, which increases to 1.95 for a slit covering the whole system. The dependence of this coefficient with the slit size noted before reflects the nonhomologous nature of the velocity dispersion gradient and mass distribution in the central parts of the remnants. Figure 1 displays the solution in the homologous case as a solid line (pure virial theorem), and it is quite evident that it does not match the FP solution obtained above.

An important question regarding the way the fundamental plane is defined here is the orientation effect. Is the resulting FP an artifact of the averaging over 100 projections? In order to address this point, we estimated the parameters r_e, σ_0 and $\langle\mu_e\rangle$ for a random direction, so that now the FP is defined based on a single direction instead of 100 as before. Then, we repeated this procedure 100 times and found that median slope for the FP is 1.31 ± 0.07, which is similar to what we found in equation (1). Also, the scatter in the FP is not significantly changed by this procedure. This result reinforces the robustness of the FP solution and guarantees that we are not introducing any vicious effect by taking the median of 100 random directions.

It is important to emphasize that the set of end products R1 to R17 occupy a region of the $(r_e, \sigma_0, \langle\mu_e\rangle)$ space corresponding to the locus of the compact galaxies in the observed FP. The covered portion of the $(\hat{E}, \hat{L})$ plane does not exhaust all the possibilities. In fact, there is a limit to the initial orbital energy of the progenitors above which there would be no merger within a Hubble time. Therefore, we may not expect to reproduce the observed range of the FP with the initial model galaxy used in this work.

In order to fulfill the observed FP, from compact to giant ellipticals, we have designed three other simulations representing an hierarchical scheme in which end-products of the former simulations merge with themselves to produce a more massive object. R6-6, R17-17, and R17-King1M represent such an hierarchy and are shown in Figure 1 as a solid triangle, a solid circle, and a solid pentagon, respectively. As can be seen, these secondary mergers are close enough to the solution of the FP obtained using only end products R1–R17. This result supports the idea that with such a scheme we might be able to reproduce the global properties of elliptical galaxies.

As already noted by several authors (e.g., Djorgovski 1992) the observed FP has a remarkable small scatter around it, which is probably associated with some regularity in the process of making elliptical galaxies. Therefore, we should expect that any simulation starting from different initial model galaxies should move by merging to the same FP as defined by R1 to R17 in order to keep the scatter of the FP as small as observed. The runs in Table 1 referred to as King-2M, R9($W0 = 8$), and R3($W0 = 8$) were designed to test this hypothesis. Figure 2 shows a plot similar to Figure 1 for the characteristic parameters of the end-products of these simulations.

The open triangle in Figure 2 refers to a progenitor which is homologous to our standard initial model but with mass equal to $2M$ and half-radius $2r_h$, which keeps σ_* unchanged. The remnant result by merging this progenitor with itself is displayed in Figure 2 as an open hexagon (see entry "King-2M" of Table 1). The short line which connects these points was taken parallel to the solution found before for runs R1–R17. As

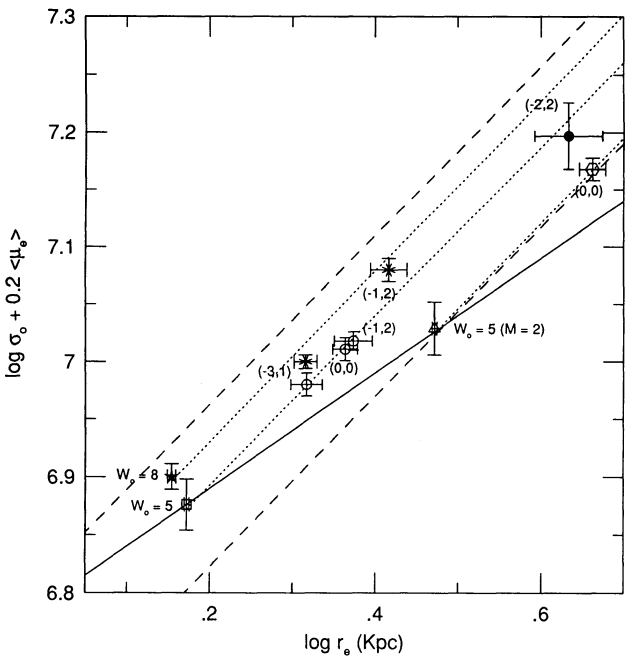

FIG. 2.—This figure shows the locus of the remnants for the runs starting from different progenitors than the "standard" one (see text). The open triangle represents an homologous progenitor with $W_0 = 5$, but with the mass and half-radius doubled; its remnant (run "King-2M") is represented by the open hexagon. The open star represents a less compact progenitor with $W_0 = 8$ and mass and half-radius identical to the "standard" one; its remnants [runs R9($W0 = 8$) and R3($W0 = 8$)] are represented by asterisks, and the remnant of a hierarchical merger of R9($W0 = 8$) with its replica is represented by the solid circle. We also plotted the "standard" progenitor (*open square*) together with some of its remnants having the same initial orbital conditions $(\hat{E}, \hat{L})$ as the other runs represented in this figure. The dotted lines starting from the three progenitors *are parallel* to the FP solution shown in Fig. 1. The two dashed lines give the *observed* 1 σ upper and lower bounds of the FP, as estimated from the FP solution obtained by de Carvalho & Djorgovski (1992) for their cluster sample. The solid line represents the virial relation passing by the "standard" progenitor.

can be seen, there is a hint that this progenitor and its remnant in fact define approximately a parallel sequence to the fitted FP.

The same seems to be true in the case where the progenitor is nonhomologous to our standard one. These are the cases of runs R9($W0 = 8$) and R3($W0 = 8$), both starting from a less concentrated King model with $W_0 = 8$, while maintaining the other parameters the same as before (except the σ_* parameter, which in this case values 1.117). Notice that in contrast to our basic model, this initial model may be more realistic when compared to real elliptical galaxies. This model is shown in Figure 2 as an open star, whereas its remnant is represented by an asterisk. Also, we can see in this figure the point that represents the remnant of R9-9($W0 = 8$) simulation (*solid circle*) exhibiting the same trend as seen before (see solid circle in Fig. 1). As in the case of the "King-2M" run, it can be seen that the line joining this progenitor and its remnant also defines a parallel sequence to the fitted FP. It is clear from this figure that the observed fundamental plane has a scatter around it which is roughly twice as big as the scatter we measured in our simulated FP. Such discrepancy could be reflecting the physical constraints on the central potential (W_0) and the mass of the primordial units from which galaxies were formed. Varying W_0 and mass we can increase the scatter of the FP and in such case the "observed" scatter restricts the range of variation of these quantities.

Two-body relaxation is a concern in all simulations and in particular in our case for it acts toward contracting the central parts of the systems and thus goes in the same sense as the deviation shown by the merger remnants relative to the expected virial relation for homologous systems. However, we know that at the, say "macroscopic" scales we are working with, the two-body relaxation acts very slowly, with timescales of order of tens of t_{rh}, the median relaxation time of the system (see, e.g., Binney & Tremaine 1987, chap. 8; see also Farouki & Salpeter 1994). We may then expect that even if some two-body relaxation has already occurred by the time we stopped our simulations, it has a negligible effect on quantities of interest as r_e and $\log \sigma_0 + 0.2\langle\mu_e\rangle$. A direct way to see if this is true is to examine the run of these quantities with the time to see how much they vary since the merger has reached equilibrium. Figure 3 shows the results of this exercise for 4 of the R1–R17 mergers, in which each of them has been projected at a random direction. In this figure we have also plotted the run of the virial ratio of the system $2T/W$, where T is the total kinetic energy of the system and W its gravitational energy, which indicate the global state of equilibrium attained by the system. As it can be seen, both quantities vary by a small amount which is well inside the projection errors, showing no systematic trend. These results are typical for all the simulations and give strong evidence that two-body relaxation do not play any significant role in the FP correlations discussed before.

That the FP correlations we found are not affected by binary relaxation is further confirmed when we perform the same analysis which was made before at $T_1 = 30 * T_{cr} + T_{per}$, where T_{per} is the time interval before the first pericenter, but now for the mergers taken at $T_2 = 15 * T_{cr} + T_{per}$. We find practically no change between the results found at T_2 and T_1, which is consistent with the discussion above: the same tight linear correlation is found, with an angular coefficient of 1.42 ± 0.08 for the $f = 0.2$ slit. It is interesting to note that this result shows that the FP developed well before the completion of the merger.

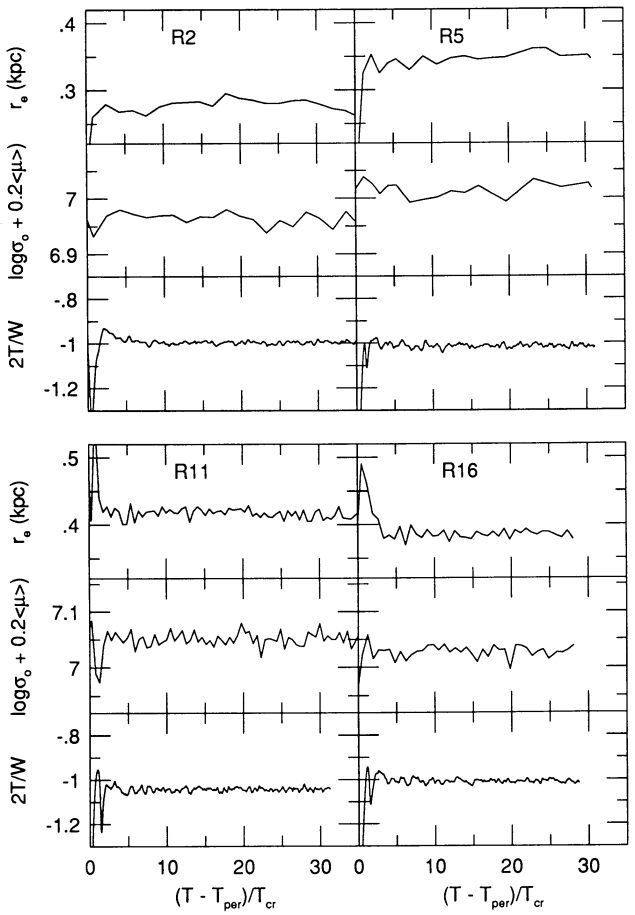

FIG. 3.—These four panels show the run of r_e and $\log \sigma_0 + 0.2\langle\mu_e\rangle$, the quantities of the FP, as a function of time counted since the first periastron (T_{per}) of the encounter, in units of the crossing time, T_{cr}, of the simulation. Each panel refers to the run which is marked at the top. In each panel we also show the run of the virial ratio $2T/W$ of the respective merger, which is helpful in indicating the relative global stage of equilibrium attained by the system.

Finally, a robustness test was done to measure how sensitive our results are to the number of particles per galaxy. These runs are referred in Table 1 as "$2NW0 = 5$" and "$3NW0 = 8$," where we doubled and tripled the number of particles, respectively. The positions of these remnants compared to the FP defined by the R1–R17 remnants are fully consistent and show that the result reached in this work is not an artifact of the low resolution, since real galaxies have a much higher number of particles. In fact, these two simulations may be directly compared to R5 and to R3($W0 = 8$) (see Table 1) and we found in both cases $\Delta \log r_e \simeq 0.02$ and $\Delta(\log \sigma_0 + 0.2\langle\mu_e\rangle) \simeq 0.02$, which is a measure of how insensitive the results are to the number of particles.

4. ON THE HOMOLOGY BETWEEN PROGENITORS AND MERGER PRODUCTS

We found that simple dissipationless merging can partly explain the observed fundamental plane for elliptical galaxies, as we described in the previous section. An important question to be addressed as a natural follow-up of this finding is about the nature of the deviation observed in the FP of elliptical galaxies with respect to the virial theorem and in what way we can use our simulation to learn about it. Indeed, under the

dissipationless assumption used here, such deviation is clearly associated with the fact that merger remnants are neither not homologous among themselves nor with their progenitors.

This deviation from homology may be more quantitatively stated by writing the scalar virial theorem in terms of the observed quantities σ_0, r_e and $\langle\mu_e\rangle$. We find

$$r_e = (C_r C_v)/(2\pi G)(\sigma_0 \Sigma_e^{-1/2})^2 , \quad (2)$$

where the coefficients C_r and C_v are defined as

$$V_v \doteq \langle v^2\rangle/\sigma_0^2 , \quad C_r \doteq R_G/r_e$$

with $\langle v^2\rangle^{1/2}$ and R_G being, respectively, the three-dimensional velocity dispersion and the gravitational radius of the system.

For a given family of equilibrium models, these two coefficients are constant so that equation (2) defines families of homologous equilibrium systems depending on the product $C_r C_v$. Note that this equation applies equally to the merger remnants as for their progenitors, since both are found in states of dynamical equilibria. In contrast, the observed relation, equation (1), may be written as

$$r_e = C_{\rm FP}(\sigma_0 \Sigma_e^{-1/2})^{\alpha} , \quad (3)$$

where $\alpha \sim 1.36$ and the constant $C_{\rm FP}$ depends on the initial equilibrium models which have been merged.

By taking into account the mass and energy variations of the merger remnants relative to their progenitors it is straightforward to relate the initial and final values of the coefficients C_r and C_v. Figure 4 shows the run of the initial-to-final ratios of the two homology coefficients as a function of $\hat{E}$ and $\hat{L}$, the normalized initial orbital energy and angular momentum of the mergers. The FP variables are also plotted. The first thing to note in this figure is the lack of any obvious dependence of these quantities on $\hat{L}$ This is due to the fact that most of the initial angular orbital momentum of the colliding galaxies is transferred to the outer parts of the merger remnant. Indeed, we found that the remnants of our simulations display negligible rotation velocity in their central regions ($r < r_e$) and that all the angular momentum is carried by the outlying material. This is consistent with results from other merger simulations (see Hernquist 1993). We have also verified that there is no significant dependence of these quantities on the structure parameter A, although the small range of variation of this variable in our simulations precludes any firm conclusion on this respect. We are thus forced to conclude that the physical parameter driving the observed values of the coefficients of the FP correlations is the initial orbital energy of the pair.

It is interesting to note that the mass distribution (C_{r_m}/C_{r_p}) seems to follow homology much better than the velocity distribution (C_{v_m}/C_{v_p}). This is even more true for the most bound initial orbits for which the ratio (C_{r_m}/C_{r_p}) $\simeq 1$, as it can be seen in Figure 4. Since it is the combination of these two non-homologies that produces the FP correlation, they somewhow reflect how the merger remnants accommodate the input energy in their central parts. In this sense, the specific value of α should be viewed as a result of the details in the merging process, and we may conjecture that it is also related to the distribution of the $\hat{E}$ at early epochs when the first galaxies started to coalesce to build hierarchically the galaxies we know today.

An independent way to study the homology question is to parameterize the major axis profile of the remnant so that possible correlations between structural parameters and the

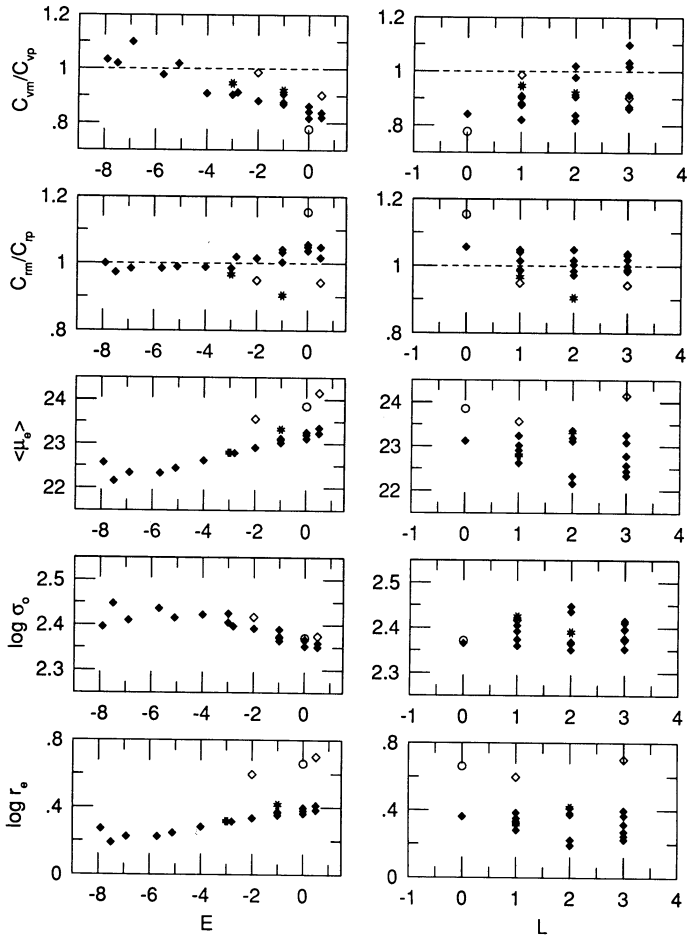

FIG. 4.—The various projected quantities related to the FP of remnants from equal progenitor mergers plotted as a function of the initial orbital energy (*left panels*) and the initial orbital angular momenta (*right panels*). Filled diamonds correspond to runs R1–R17; asterisks to runs R9($W0 = 8$) and R3($W0 = 8$). The open diamonds correspond to R6-6 and R17-17, and the open circle to the run "King-2M."

initial conditions can be investigated. As we pointed out before, Caon et al. (1993) obtain better fits to the major-axis luminosity profiles of a sample of elliptical galaxies using an $r^{1/n}$ law, as opposed to an $r^{1/4}$ law. The best values for the parameter n for their fits vary from 2 to 20 and are correlated to the effective radius of the galaxies. An important caveat is that such methodology should be applied with some precaution since S0 galaxies ($r^{1/4}$ bulge + an exponential disk) could be fitted to an $r^{1/n}$ law with different values of n reflecting probably different disk/bulge ratios instead of nonhomology. However, it is still an important result for it shows that the traditional view by which elliptical galaxies are homologous objects (at least in their luminosity distribution), described by an $r^{1/4}$ law may not be the case. In order to see if a similar effect was present in our merger remnant (and in this case we are not polluted by a disk component) we fit the $r^{1/n}$ law to the mean major-axis mass density profile. As before this mean profile was obtained from 100 profiles taken from randomly distributed directions. The fitting interval chosen was from 0.5 kpc ($\sim 10\epsilon$) to $1r_e$. The parameter n obtained from these fits varies from 1.2 to 3.4 and it correlates with r_e. In other words, n is correlated to the deviation between the FP and the virial relation in the sense that large deviations correspond to large n.

This last result is also consistent with those reported by Caon et al. (1993).

The nonhomologous nature of remnants of dissipationless mergers was studied in earlier numerical experiments (e.g., Miller & Smith 1979; White 1980; FSD; Navarro 1989). FSD noted that the nonhomologous nature of *hierarchical* parabolic merging of similar galaxies is capable of correctly explaining the Faber-Jackson relation. Moreover, as can be shown from their results, the FP itself may be explained in the same way. Although with much poorer simulations, FSD have shown that for parabolic encounters the half-mass radius of the merger remnants, R_{50}, grows proportional to the mass of the remnant, whereas the radius containing 10% of the mass grows more slowly, $R_{10} \propto M^p$, with $p \simeq 0.3$, and the average velocity dispersion within R_{10}, $\sigma_{10} \propto M^q$, with $q \simeq 0.25$, which is the Faber-Jackson relation, Since the projected half-mass radius, r_e, must correspond to some spatial radius R_X encompassing a fraction $10\% < X < 50\%$ of the mass, we may hint that $r_e \propto M^s$, with $s \simeq 0.6$, which is the mean between the two extreme values. Substituting these relations in the scalar virial theorem, we find $r_e \propto \sigma_0^{2\alpha} \bar{\Sigma}_e^{-\beta}$, with $\alpha \simeq 0.80$ and $\beta \simeq 0.90$ (or $\log r_e = 1.6(\log \sigma_0 + 0.36\langle\mu_e\rangle) + C$, which is consistent with the observed FP. We stress that the FSD simulations are restricted to parabolic encounters, although Navarro (1989, 1990) already gave hints that these results may be extended to elliptical or hyperbolic encounters.

5. CONCLUSIONS

In this work we aimed to measure the usual set of quantities which constitute the so-called fundamental plane (FP) correlations of elliptical galaxies (e.g., r_e, σ_0, $\langle\mu_e\rangle$) for a sample of N-body simulations of mergers of identical galaxies. In doing so, we have shown that merger remnants obey a relation which is very close to the observed FP correlation. Actually, by merging a first generation of merger remnants with themselves we found that the FP is still preserved. These results suggest an hierarchical merging scheme, where remnants are merged among themselves to produce successive merger remnants generations, extending the FP relation over the entire $(r_e, \sigma_0, \langle\mu_e\rangle)$ space of observed elliptical galaxies.

These results indicate that the FP correlations may be originated by pure gravitational processes rather than by dissipative gas processes as is commonly accepted (e.g., Faber 1987; Djorgovski 1988). Indeed, we found that for our dissipationless merger remnants, it is the nonhomologous nature of both the velocity and mass distributions in their central region ($r < r_e$) that is responsible for the small departure from the homology prediction, which is characteristic of the observed FP correlation.

We emphasize that it is the central velocity distribution and not the mass (luminosity) distribution that strongest deviates from homology. Thus, although there is some observational evidence (also seen in our simulations) that the *central* luminosity distribution of elliptical galaxies is not homologous (Caon et al. 1993), it is the observation of their central velocity distribution that may fully reveal this effect. This would be, however, a much harder observational task. It is interesting to note that we found no significant homology deviation when we use the global projected dispersion velocity of the merger remnant instead of its central value: this reinforces the view that nonhomology effects concern only the central parts of the remnants. Besides, we also find that the nonhomologous deviation of a merger remnant from its progenitor is nearly exclusively a function of the initial energy of the pair.

We find that different initial progenitors produce different families of merger remnants, all of them obeying relations similar to the FP correlation but displaced by different amounts. This could be indicative that the central potential and mass of the primordial units did not have a wide distribution, otherwise the scatter of the observed FP would be much larger.

We argue that under the assumptions presented along this paper, elliptical galaxies (or at least those living in clusters of galaxies), could be generated in a dissipationless hierarchical merging scheme. However, it is important to emphasize that although we explain the coefficients involved in the FP definition, the observed scatter in this relation is still not well understood. We could either claim for a constraint on W_0 and mass of the first generation galaxies or that dissipation processes contributed to the increasing of the scatter without changing the general trend.

As stressed before, our experiments do not explicitly include any dark matter component. The simulations presented here correspond to galaxies which have already spiralled in through their common dark matter halo, so that at the initial conditions their visible parts are nearly touching. However, as we have shown, the variation of orbits leaves the end products on the same fundamental plane as they began. It is likely that adding some dark matter at large radii would mainly act to change the effective orbital parameters but in any case the outcome of the collisions would leave the remnant on the FP. In this sense, we are confident that there is indeed no loss of generality in neglecting the effects of any dark matter halo component. We are currently investigating the effect of dark matter on the FP but under different initial conditions. This will be a subject for a future contribution.

We thank Eraldo Marinho, Gastão B. Lima Neto, J. Smith, Francoise Combes, and S. G. Djorgovski for helpful comments. We would like to thank the anonymous referee for very helpful comments and suggestions which helped to improve the paper. R. R. de Carvalho was supported by FAPESP, Proc. No. 92/2686-9. H. V. Capelato was partially supported by CNPq, Proc. No. 301225/80.

REFERENCES

Barnes, J., & Hut, P. 1986, Nature, 324, 446
Bender, R., Burstein, D., & Faber, S. M. 1992, ApJ, 399, 462
Bertin, G., & Stiavelli, M. 1993, Rep. Prog. Phys., 56, 493
Binney, J., & Tremaine, S. 1987, Galactic Dynamics (Princeton: Princeton Univ. Press)
Burstein, D., Davies, R. L., Dressler, A., Faber, S. M., Stone, R. P. S., Lynden-Bell, D., Terlevich, R. J., & Wegner, G. 1987, ApJS, 64, 601
Caon, N., Capaccioli, M., & D'Onofrio, M. 1993, MNRAS, 265, 1013
Davies, R. L., Burstein, D., Dressler, A., Faber, S. M., Lynden-Bell, D., Terlevich, R. J., & Wegner, G. 1987, ApJS, 64, 581
de Carvalho, R. R., & Djorgovski, S. G. 1992, ApJ, 389, L41
Djorgovski, S. G. 1988, in Proc. Moriond Astrophysics Workshop, Starbursts and Galaxy Evolution, ed. T. X. Thuan et al. (Gif sur Yvette: Editions Frontières), 549
———. 1992, in ASP Conf. Ser., No. 24, Cosmology and Large-Scale Structure in the Universe, ed. R. R. de Carvalho (San Francisco: ASP), 19

Djorgovski, S. G., & Davis, M. 1987, ApJ, 313, 59
Djorgovski, S. G., & de Carvalho, R. R. 1990, in Windows on Galaxies, ed. G. Fabbiano et al. (Dordrecht: Kluwer), 9
Djorgovski, S. G., & Santiago, B. X. 1993, in Proc. ESO/EIPC Workshop, ESO Conf. & Workshop Proc. 45, Structure, Dynamics and Chemical Evolution of Elliptical Galaxies, ed. I. J. Danziger, W. W. Zeilinger, & K. Kjar (Garching: ESO), 59
Dressler, A., Lynden-Bell, D., Burstein, D., Davies, R. L., Faber, S., Terlevich, R. J., & Wegner, G. 1987, ApJ, 313, 42
Dubinski, J. 1988, MS thesis, Univ. of Toronto
Faber, S., Dressler, A., Davies, R. L., Burstein, D., Lynden-Bell, D., Terlevich, R. J., & Wegner, G. 1987, in Nearly Normal Galaxies, ed. S. Faber (New York: Springer), 175
Farouki, R. T., & Salpeter, E. E. 1994, ApJ, 427, 676
Farouki, R. T., & Shapiro, S. L. 1982, ApJ, 259, 103
Farouki, R. T., Shapiro, S. L., & Duncan, M. J. 1983, ApJ, 265, 597
Hernquist, L. 1993, ApJ, 409, 548
Hernquist, L., Spergel, D. N., & Heyl, J. S. 1993, ApJ, 416, 415
King, I. R. 1966, AJ, 71, 64
Miller, R. H., & Smith, B. F. 1979, ApJ, 227, 785
Navarro, J. 1989, MNRAS, 239, 257
———. 1990, MNRAS, 242, 311
Pearce, F. R., Thomas, P. A., & Couchman, H. M. P. 1993, MNRAS, 264, 497
Recillas-Cruz, E., Carrasco, L., Serrano, A., & Cruz-Gonzáles, I. 1991, AA, 249, 312
Renzini, A., & Ciotti, L. 1993, ApJ, 416, L49
White, S. D. M. 1980, MNRAS, 191, 1P